❚ Photoredox Catalysis

Amphiphilic Polymeric Nanoparticles for Photoredox Catalysis in Water

Fabian Eisenreich, E. W. Meijer, and Anja R. A. Palmans*[a]

Abstract: Photoredox catalysis has recently emerged as a powerful synthesis tool in organic and polymer chemistry. In contrast to the great achievements realized in organic solvents, performing photocatalytic processes efficiently in aqueous media encounters several challenges. Here, it is presented how amphiphilic single-chain polymeric nanoparticles (SCPNs) can be utilized as small reactors to conduct light-driven chemical reactions in water. By incorporating a phenothiazine (PTH) catalyst into the polymeric scaffold, metal-free reduction and C—C cross-coupling reactions can be carried out upon exposure to UV light under ambient conditions. The versatility of this approach is underlined by a large substrate scope, tolerance towards oxygen, and excellent recyclability. This approach thereby contributes to a sustainable and green way of implementing photoredox catalysis.

Introduction

Photoredox catalysis has recently become a flourishing field in modern organic chemistry as it paves the way for novel modes of reactions under mild and biocompatible conditions (i.e., ambient temperature and non-invasive light irradiation).[1–4] Light energy is used as a fuel to accelerate chemical transformations by single-electron redox processes, thereby giving rise to well-controlled and improved synthetic procedures. Thus far, tremendous progress has been achieved to synthesize value-added products efficiently in organic solvents. Aside from these advances, there is a strong interest in the field of nano-medicine or other biological applications for the development of photoredox-active catalyst systems that can be operated in pure water. The ability to perform modern chemical reactions in aqueous media together with effective recycling strategies for catalysts represent keystones for sustainable and green chemistry.[5,6] To this end, nature's fascinating repertoire of tools to perform chemical transformations with tremendous accuracy and reliability (e.g., enzymatic reactions) can serve as a precious source of inspiration. In many enzymes, hydrophobic domains that are shielded from the aqueous environment based on well-defined tertiary architectures provide an anchor point for efficient catalysis. This precise compartmentalization of catalytic sites has the additional advantage to result in a dramatic elevation of catalytic activity and selectivity.
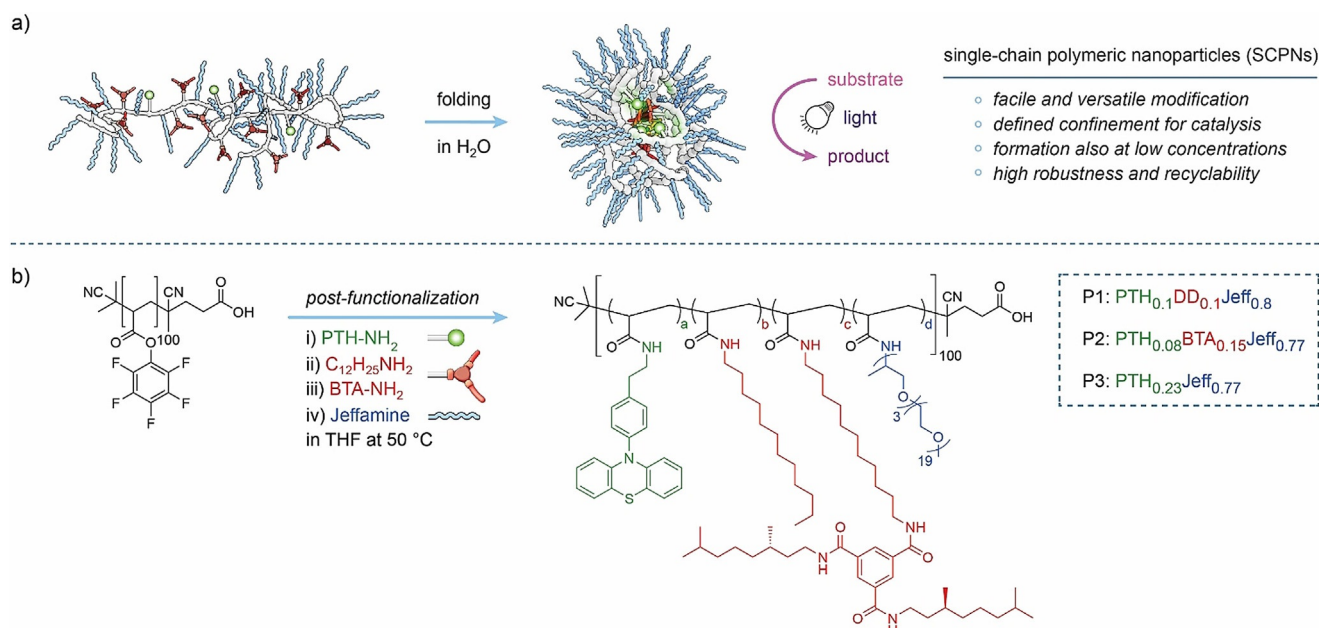
Hitherto, examples for photoredox catalysis in pure water are scarce and mostly rely on water-soluble ruthenium complexes[7,8] or micellar approaches.[9,10] For instance, in pioneering work of Lipshutz and co-workers,[11] tailor-made micelles have been applied as reaction compartments for efficient catalysis in water. With the aid of an iridium-based photocatalyst covalently attached to an amphiphilic micelle-forming reagent, alkenes were functionalized with sulfonyl groups.[12] By capitalizing on the recyclability of their catalyst system, the net usage of iridium was reduced to the level of ppm over several reaction cycles. Recently, the group of König has impressively shown that micellar assemblies can be utilized to activate stable carbon–chlorine bonds with light for various chemical transformations, such as reduction, cross-coupling, and cyclization reactions.[13] Moreover, the generation of hydrated electrons as versatile super-reductants was thoroughly studied by the group of Goez based on photoredox processes involving ruthenium complexes and the support of micelle compartmentalization.[14–16]

In these seminal contributions in the field of photoredox catalysis in aqueous media, the predominant utilization of metal catalysts typically unfold their reactivity in the excited triplet state, thus requiring oxygen-free conditions. Furthermore, the utility and benefits of immobilizing a photoredox catalyst onto amphiphilic polymer-based systems have not been explored to date in this regard. By linking a catalytic unit to a polymeric support several crucial advantages can be unlocked, namely high robustness, facile separation and opportunities for recycling, and restricted catalyst leaking.[17,18] The contamination of reaction products with traces of catalyst can

[a] *Dr. F. Eisenreich, Prof. Dr. E. W. Meijer, Prof. Dr. A. R. A. Palmans*
Laboratory of Macromolecular and Organic Chemistry
Institute for Complex Molecular Systems, Department of
Chemical Engineering and Chemistry, Eindhoven University of Technology
P.O. Box 513, 5600 MB Eindhoven (The Netherlands)
E-mail: a.palmans@tue.nl

Chemistry–A European Journal

Full Paper
doi.org/10.1002/chem.202001767

**Chemistry
Europe**
European Chemical
Societies Publishing

Figure 1. Photoredox-active single-chain polymeric nanoparticles: a) Illustration of the intramolecular hydrophobic collapse of an individual chain to a nanoparticle in water, furnishing a nonpolar interior as platform for photoredox catalysis. b) Post-functionalization of poly(pentafluorophenyl) acrylate by the sequential addition of amine-bearing compounds to yield the catalytically active polymers **P1**–**P3**.

thus be prevented, which is particularly important for biomedical[19] or microelectronic applications.[20]

In the late 90s, Bergbreiter and co-workers reported on the high activity and simple recovery of water-soluble polymer-bound catalysts.[21,22] Beyond that, various synthetic macromolecules, such as star polymers[23–25] and dendrimers,[26,27] have been created with the aim to isolate incorporated catalytic units from the aqueous surroundings.[28–30] Dynamic and cross-linked micelles,[31–36] nanogels,[37,38] as well as various polymer-supports[39,40] have also been investigated in detail to realize efficient catalysis in water.

In our group, we have established that both, organocatalytic as well as transition-metal-based reactions, proceed well in water when the catalytically active sites are shielded by amphiphilic polymer chains that fold around the catalyst to form single-chain polymeric nanoparticles (SCPNs; see Figure 1 a).[41–43] As a result, stable, structured, and hydrophobic interiors are created, in which reactions can be performed that are typically not compatible with water due to the lack of solubility of either the substrate or the catalyst. While most of the reported catalytic processes with SCPNs are conducted thermally, it would be highly advantageous to gain control over a catalytic reaction with light as an external trigger. With the aim to avoid precious transition metal catalysts (e.g., iridium and ruthenium complexes) we chose 10-phenylphenothiazine (PTH) as an organic photocatalyst for our study. Hawker and Read de Alaniz et al. have shown that PTH efficiently facilitates dehalogenation reactions[44,45] and C–C cross couplings.[45] PTH and derivatives thereof are also known to catalyze controlled radical polymerizations of various monomers.[46–50] Moreover, PTH bound to a hydrophobic polymer-support was successfully applied in photocatalysis and recycling studies in organic media.[51]

Here, we describe the use of SCPNs as a stable and recyclable platform to perform metal-free photoredox catalysis in water. The devised method is simple to operate as cheap and commercially available light-emitting diodes (LEDs) are employed as light sources. More importantly, the catalytic reactions take place at ambient temperature and in the presence of air oxygen, representing prerequisites for potential biological applications.

Results and Discussion

Molecular design, synthesis, and characterization of photoredox-active SCPNs

We designed three, differently substituted, amphiphilic polymers (**P1**–**P3**, Figure 1 b) that differ in the amount of hydrophobic alkyl residues (**P1** versus **P3**), the presence of structuring moieties (benzene-1,3,5-tricarboxamide, BTA, **P2**) and the amount of photoredox catalyst PTH ($\approx 10\%$ in **P1** and **P2**, and $\approx 23\%$ in **P3**). In all cases, we selected long polyetheramine-based chains, so-called Jeffamine®M-1000 (Jeff), to impart sufficient water-solubility. In order to covalently attach the catalytic unit to the polymer backbone, we slightly modified the chemical structure of PTH by introducing an ethylamine linker at the 4-position of the phenyl group. To increase the number of hydrophobic side groups that furnish the inner compartments of the SCPNs, linear dodecyl chains were selected for **P1**.[52] The use of chiral, non-racemic BTA ((S)-BTA) units permits to investigate the structural integrity of the SCPNs under operating conditions (**P2**).[42] These moieties are capable of forming helical stacks due to threefold hydrogen bonding[41,53] and thus render a structuring element within the nanoparticle cores. The supramolecular helical assemblies can be analyzed by cir-

Chemistry–A European Journal | Full Paper
doi.org/10.1002/chem.202001767

Chemistry
Europe
European Chemical
Societies Publishing

cular dichroism (CD) spectroscopy and hence provide the means to probe the integrity of the inner composition upon exposure to the reaction conditions. Polymer **P3** was solely functionalized with PTH, but in relatively high amounts, and Jeffamine. Overall, these three polymers were selected to investigate whether composition and catalyst loading of the polymer affect the catalytic performance of SCPNs for light-mediated reactions.

To avoid differences in the degree of polymerization and molar mass dispersity in the three polymers, we chose a post-functionalization approach starting from poly(pentafluorophenyl) acrylate to prepare the amphiphilic polymers.[52] This polymer with activated ester pendants can be randomly functionalized with various amine-bearing compounds as side groups (Figure 1b),[54] making the stepwise synthesis of SCPNs easy and versatile. It is important that the distribution of the hydrophobic moieties is random since this ensures an intramolecular hydrophobic collapse in water and hereby the formation of nanoparticles from a single polymer chain.[52, 55–57]

Poly(pentafluorophenyl) acrylate with an average degree of polymerization of 100 and a molar mass dispersity Đ of 1.17 (determined by SEC, size exclusion chromatography, in THF calibrated with polystyrene standards) was obtained after reversible addition-fragmentation chain-transfer (RAFT) polymerization of pentafluorophenyl acrylate and subsequent removal of the RAFT end group.[52] Each sequential post-modification step was monitored by ^{19}F NMR spectroscopy and the degree of amine-functionalization was determined by comparing the signals originating from the released pentafluorophenol and the polymer precursor (see Figures S1–S3 in the Supporting Information). Thereby, the set of three differently substituted amphiphilic polymers (**P1**-**P3**) was synthesized and fully characterized. The modified polymers have a theoretical molecular weight of ca. 90 kDa and molar mass dispersities of Đ = 1.11–1.13 (SEC in DMF with LiBr, calibrated with poly(ethyleneoxide) standards).

Dynamic light scattering (DLS) measurements revealed on the one hand that the hydrodynamic radii of the nanoparticles of **P1** and **P3** are 5.2 and 5.6 nm in water, respectively, which is the typical regime for nanoparticles consisting of individual polymer strands[52] (see Figure S4 in the Supporting Information). Interestingly, the presence of the aromatic PTH moieties appears to suffice to induce an intramolecular hydrophobic collapse into a SCPN. On the other hand, nanoparticles of **P2** show a slightly higher radius of 6.5 nm, a result of interactions between nanoparticles and the formation of presumably dimeric aggregates. This is consistent with our previous results where BTA loadings above 10% were found to induce some clustering of the polymer chains.[52]
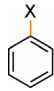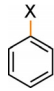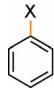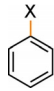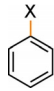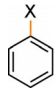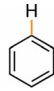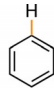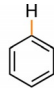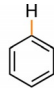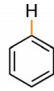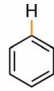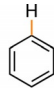
The optical properties of the polymers were studied via UV/vis spectroscopy in water as well as organic solvent (i.e., acetonitrile; see Figure S5 in the Supporting Information). The UV/Vis spectra show in both solvents the typical absorption bands of the incorporated PTH catalyst[58] with maxima at around 258 and 320 nm, indicating the successful incorporation of the photocatalyst within the polymer scaffold (in accordance with NMR spectroscopy, see Figures S6–S8 in the Supporting Information).

Optimization of reduction conditions for benzene halides

With the characterized polymers in hand, we investigated their catalytic activity towards the light-driven dehalogenation of benzene halides. Previously reported mechanistic investigations showed that the working principle is based on a single-electron-transfer from the highly reducing excited catalyst to the substrate, followed by a homolytic cleavage of the carbon-halide bond and the formation of a benzene radical.[44] The presence of a tertiary amine base is paramount to guarantee a successful outcome as it regenerates the photoredox catalyst and also acts as the proton source to yield the reduced benzene compound. The catalytic reactivity of PTH primarily originates from its excited singlet state and not from its oxygen-sensitive triplet state, thus reductions can be performed without excluding oxygen.

First, we optimized the reaction conditions for the dehalogenation of iodobenzene with the aim to reach full conversion aft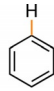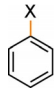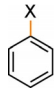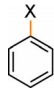er 1 h of irradiation with a 385 nm LED (see Figure S9 in the Supporting Information for the general reaction setup). For the optimization we used 10 mg of **P1** in 0.8 mL of deionized water, which corresponds to a polymer concentration of 140 μM and catalyst loading of 4 mol%, and examined several tertiary amines (Table 1). We observed that a quantitative conversion to benzene was obtained with triethylamine (see entry 1 in Table 1 and Figure S10 in the Supporting Information). The formation of benzene decreased with an increasing

Table 1. Screening of different tertiary amines for the light-driven dehalogenation of benzene halides in water.

Entry	Substrate	Deviation from procedure[a]	Irradiation time	Conversion[c,d]
1	**1**	as shown	1 h	99%
2	**1**	NiPr$_2$Et	1 h	85%
3	**1**	NCyMe$_2$	1 h	80%
4	**1**	NPr$_3$	1 h	51%
5	**1**	NBu$_3$	1 h	27%
6	**1**	NHex$_3$	1 h	13%
7	**2**	as shown	24 h	99%
8	**3**	as shown	24 h	40%
9	**1**	no NEt$_3$, no **P1**	1 h	0%
10	**1**	no NEt$_3$	1 h	traces
11	**1**	no **P1**	1 h	traces
12	**1**	no light	1 h	0%
13	**1**	blue-light LED (405 nm)	1 h	45%
14	**1**	sun light	7 h	17%
15	**1**	in CDCl$_3$[b]	1 h	0%
16	**1**	in [D$_8$]THF[b]	1 h	0%
17	**1**	in CD$_3$CN[b]	1 h	41%

[a] Standard procedure: 30 μmol (1 equiv.) of substrate, 5 equiv. NEt$_3$, and 10 mg of **P1** were taken up in 0.8 mL of deionized water and the mixture was irradiated with a 385 nm LED. After the indicated time, the mixture was extracted with CDCl$_3$ and the conversion was determined by ^1H NMR spectroscopy. [b] The solution was analyzed directly by ^1H NMR spectroscopy without extraction. [c] A conversion of 99% indicates quantitative conversion by NMR. [d] When conversion was below 99% only starting material remained, no side products were observed.

Chemistry–A European Journal

Full Paper
doi.org/10.1002/chem.202001767

Chemistry Europe
European Chemical
Societies Publishing

hydrophobicity of the amines (see entries 2–6 in Table 1). We also applied inherently less reactive bromo- and chlorobenzene as substrates under these conditions and measured conversions of 99% and 40%, respectively, after light exposure of 24 h (see entries 7 and 8 in Table 1). Importantly, no side products were detected during the light-driven dehalogenation of benzene derivatives **1**–**3**. In control experiments, we validated that product formation is indeed only taking place when the photoredox-active nanoparticles and triethylamine are simultaneously present in combination with the required light activation (see entries 9–12 in Table 1). Instead of using UV light (385 nm) it is also feasible to perform the photocatalytic reaction with a blue-light LED (405 nm) or even sunlight, thereby contributing to sustainable and green chemistry (see entries 13 and 14 in Table 1).

In order to substantiate the importance of the formation of SCPNs acting as nanoreactors, we executed the reduction of iodobenzene in organic solvents, in which the hydrophobic collapse and thus nanoparticle generation is precluded. Under otherwise identical conditions, either no product was detected (in deuterated chloroform and tetrahydrofuran) or moderate yields were obtained (in deuterated acetonitrile; see entries 15–17 in Table 1). This emphasizes the value of providing a defined nanocompartment for catalysis—similar to enzymes—in which high local concentrations of reagents lead to an acceleration of product formation.

Investigation of substrate scope and tolerance towards functional groups

Based on these promising initial results, we further checked for the substrate scope of this chemical transformation as well as potential differences between the set of polymers. To this end, we merely focused on iodobenzene derivatives due to their relatively high reactivity (Scheme 1). It turned out that a variety of functional groups are tolerated, ranging from electron-poor derivatives (substrates **4**–**6**) that expectedly gave higher conversions than electron-rich derivatives (substrates **7**–**10**) to heterocyclic compounds (substrates **11**–**13**). By comparing the individual results of **P1**-**P3** for each substrate, slight deviations can be identified, while they all follow the same trend in compliance with the reactivity of the iodobenzene derivatives. Contrary to our expectations, the use of polymer **P3** with the highest number of catalysts attached (catalyst loading of 8 mol% under the applied conditions) resulted in the highest product formation for compounds **8** and **10**, but not for the others. Interestingly, polymer **P2**, which is modified with the fewest PTH functionalities (catalyst loading of 3 mol%), showed the best performance for substrates **6** and **11**. By employing an acidic compound, such as 4-iodophenol **9**, polymer **P1** gave the best result, which in turn generally yielded the lowest conversions for the other starting materials. Although the reduction of 2-iodobenzoic acid **5** was carried out in deuterated water, no signals for the reduced deuterated product were detected by NMR spectroscopy (see Figure S11 in the Supporting Information). This is consistent with the proposed mechanism stating that the tertiary amine is the primary proton source and not
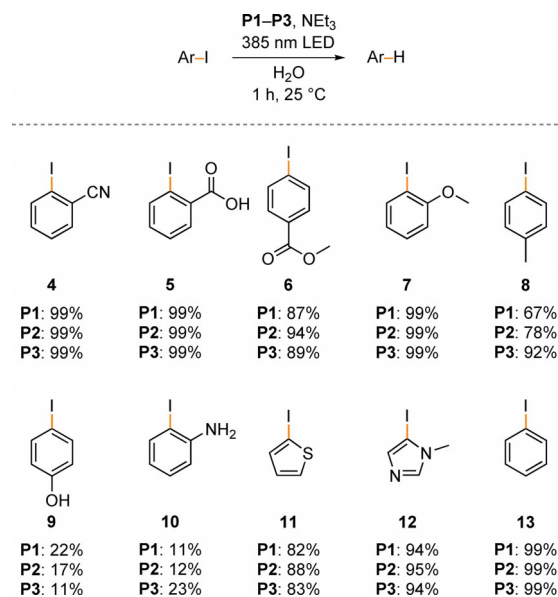
Scheme 1. Illustration of the reaction scope for the dehalogenation of differently substituted (hetero)aryl iodides. The indicated conversions are average results of at least two experiments following the general protocol. The reduction of 2-iodobenzoic acid **5** was carried out in deuterated water.
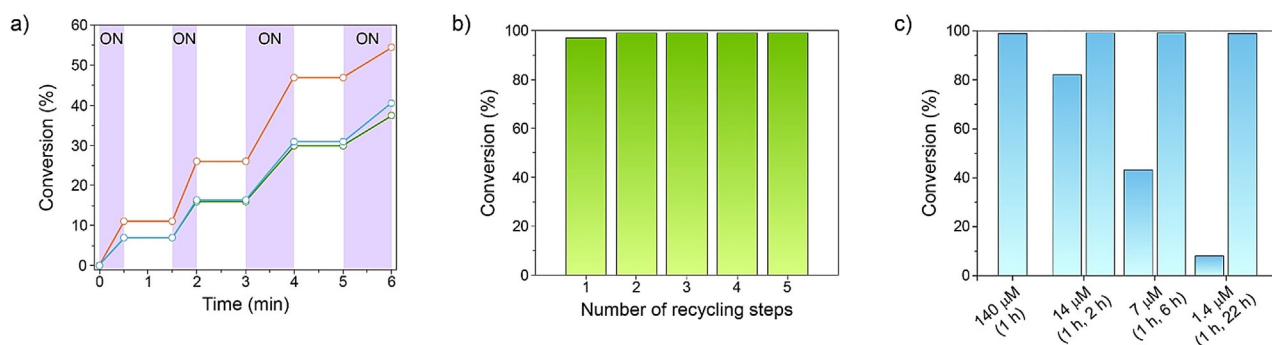
the solvent.[44] Remaining starting material can be completely converted by extending the illumination period if needed, hence product purification steps by column chromatography are not required.

Overall, polymers **P1**–**P3** display a high activity for the light-mediated reduction of (hetero)aryl iodides in water based on the (almost) quantitative conversion of many substrates after 1 h. As examples in organic solvents under comparable conditions require longer reaction times,[44,59,60] it becomes apparent that the compartmentalization and thus high local concentration of reagents in SCPNs accelerate the product formation.

In a previous report on SCPNs, it was shown that the presence of BTA groups within the nanoparticles was paramount to render a proline catalyzed aldol reaction successful.[42] The study presented here, however, displays that the catalytic performance of the PTH photoredox catalyst is only marginally influenced by the composition of the SCPNs. As a positive consequence, the functionalization of the polymer backbone can be simplified, as demonstrated with **P3**, by only attaching the catalytic moiety and Jeffamine for water-solubility. Elaborate synthesis of additional pendant groups, such as (S)-BTA, is thus not required. Moreover, the differences in catalyst loading, which ranged between 3–8 mol% depending on the applied polymer, did not result in a significantly altered catalytic efficiency. This strongly indicates that only a fraction of the catalyst was simultaneously excited with light to populate the reactive excited state.

Temporal control, recyclability, and concentration study

Benzoic acid derivative **5** shows near complete conversion to benzoic acid in 1 h for all polymers **P1**–**P3**. In order to assess differences in the activity of the different polymer catalysts for

Chemistry–A European Journal

Full Paper
doi.org/10.1002/chem.202001767

**Chemistry
Europe**
European Chemical
Societies Publishing

Figure 2. Experiments demonstrating the versatility of the photoredox-active SCPNs: a) Substrate conversion over time during the dehalogenation reaction of 2-iodobenzoic acid **5** in the presence of triethylamine and polymer **P1** (orange line), **P2** (blue line), and **P3** (green line) in deuterated water. The 385 nm LED was alternatingly turned ON (purple background) for 0.5 or 1 min and switched OFF for 1 min. Each experiment was performed at least in duplicate. b) Recycling experiment based on the consecutive dehalogenation reaction of 2-iodobenzonitrile **4** in the presence of triethylamine and polymer **P1** in water. c) Dehalogenation reaction of 2-iodobenzoic acid **5** in the presence of triethylamine and polymer **P3** with different polymer concentrations and reaction times in deuterated water.

this substrate, we performed a typical step experiment. Herein, the conversion of **5** to benzoic acid is followed as a function of time while the light source is repetitively turned ON and OFF (see Figure 2a and Figure S12 in the Supporting Information). On the one hand, the results for this experiment underline that the dehalogenation reaction is only taking place when the mixture is irradiated with light and paused when the LED is switched OFF, thereby giving rise to a temporally well-controlled catalytic process. On the other hand, we observe that the use of **P1** yielded the highest conversion (55% after in total 3 min of irradiation) compared to **P2** (41%) and **P3** (38%).

We were furthermore interested in the possibility of recycling the photoredox-active SCPNs and thus performed a series of consecutive reactions using polymer **P1** and 2-iodobenzonitrile **4** as the substrate (see Figure 2b and Figure S13 in the Supporting Information). Using SCPNs has the advantage that organic compounds can conveniently be extracted from the aqueous phase with diethyl ether, while the polymer remains in the water layer.[42] After each run, we extracted the water mixture accordingly, determined the conversion by ^{1}H NMR spectroscopy, charged the polymer-containing aqueous solution with **4** and fresh triethylamine, and illuminated it again with light of 385 nm for 1 h.

The dehalogenation reactions were quantitative after each run and we did not observe a decrease of reactivity over the course of five recycling steps. These results highlight the robustness and reusability of these PTH-comprising SCPNs.

Another benefit of SCPNs, besides their recyclability, is that the nanoparticles also form at highly diluted concentrations. This could be beneficial in those cases where highly dilute conditions are desired. We capitalized on this by performing the reduction of 2-iodobenzoic acid **5** with varying amounts of polymer **P3** and observed catalytic activity even at a polymer concentration of 1.4 μM, which corresponds to a catalyst loading of 0.08 mol% (see Figure 2c). Even at this very low catalyst loading, a near quantitative conversion of 99% was observed after 22 h.

Investigation of nanoparticle stability by DLS and CD measurements

At this point, we wanted to confirm that the nanoparticles are in fact stable under the reaction conditions applied. DLS measurements showed marginally increased hydrodynamic radii of the formed SCPNs in the presence of high excess of triethylamine and subsequently added 4-iodophenol **9**, which can be attributed to a swelling effect of the nanoparticles (see Figure S4 in the Supporting Information). We additionally analyzed an aqueous solution of polymer **P2** by circular dichroism spectroscopy and detected a negative CD effect originating from the formation of helical stacks of the BTA pendants within the nanoparticles (Figure 3). This supramolecular assembly can be used as a molecular probe to investigate whether the inner composition remains intact or is disturbed by the accommodation of substrate. To this end, we added again high excess of triethylamine to the aqueous spectroscopy solution and as a result neither intensity nor shape of the CD signal
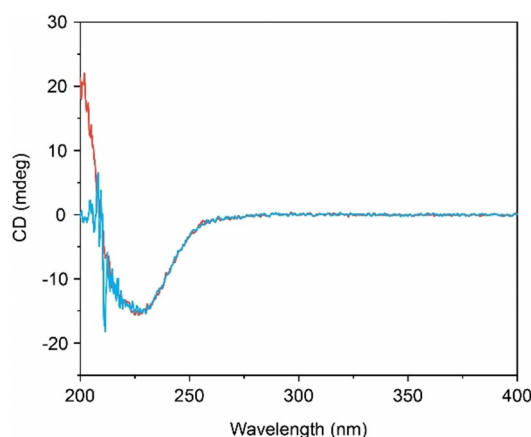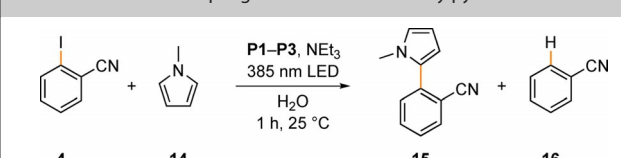

Figure 3. CD spectra of a solution of **P2** in water ($c = 0.1$ mg mL^{-1}, $V = 3$ mL) before (red curve) and after the addition of 1 μL of triethylamine (ca. 2300 equiv., blue curve) at 20 °C. The negative CD signal, which originates from supramolecular helical stacks of the BTA units[41,53] within the nanoparticle core, is not affected by the presence of triethylamine.

Chemistry–A European Journal

Full Paper
doi.org/10.1002/chem.202001767

Chemistry Europe
European Chemical
Societies Publishing

were impaired, indicating that the nanoparticles' inner structure remains untouched.

Cross-coupling reaction with *N*-methylpyrrole

Lastly, we explored the C—C cross coupling between 2-iodobenzonitrile **4** and electron-rich *N*-methylpyrrole **14** to expand the versatility of our photoredox-active SCPNs (see Table 2 and Figure S14 in the Supporting Information). Previously reported protocols in organic media typically use high excess of pyrrole (25–50 equivalents)[45,59,61] in order to trap the generated benzene radical efficiently and thus compete with the reduction pathway. However, we envisioned that the quantity of coupling partner and thereby the amount of waste can be reduced significantly by benefiting from the high local concentrations of reagents within the hydrophobic compartment created by the SCPNs. Indeed, we achieved comparable conversions by only adding 5 equivalents of **14** to the aqueous mixture (see entries 1–3 in Table 2). In addition, the reaction time of 1 h is notably shorter compared to the reaction time reported in literature.[59] In order to reduce the formation of the dehalogenated side product **16**, we applied less triethylamine, on the one hand, as it is the major proton source for the reduction pathway[44] (see entry 4 in Table 2). On the other hand, we doubled the amount of **14** added to the reaction (see entry 5 in Table 2). Both strategies led to a slight increase of the desired coupling product **15**.

Table 2. C—C cross-coupling reaction with *N*-methylpyrrole.

Entry	Polymer	NEt₃ (equiv.)	14 (equiv.)	Conversion	Ratio 15/16
1	**P1**	5	5	99%	64:36
2	**P2**	5	5	99%	65:35
3	**P3**	5	5	99%	66:34
4	**P1**	1	5	99%	78:22
5	**P1**	5	10	99%	70:30

Conclusions

In summary, we utilized robust and easily recyclable single-chain polymeric nanoparticles for efficient and well-controlled metal-free photoredox catalysis in water under ambient conditions (including the presence of air oxygen). The modular and facile synthetic approach to prepare SCPNs allows to study a set of differently substituted amphiphilic polymers, which were functionalized with a phenothiazine group as the photocatalytic unit. The SCPNs were successfully employed as tailor-made nanoreactors for the reduction of (hetero)aryl halides upon irradiation with light of 385 nm, thereby showing a high tolerance towards a wide array of functional groups. In addition, the nanoparticles show a pronounced stability even upon ex-

posure to high excess of reagents and still act as catalysts at low micromolar concentrations. On this basis, we applied this reaction setup for an arylation reaction with an electron-rich pyrrole. By providing hydrophobic compartments and thus high local concentrations of reagents within the nanoparticles, an acceleration of product formation could be observed. As a result, most of the light-driven reactions were (almost) completed within 1 h, which is generally faster compared to examples in organic media under similar conditions.[44,59,60] By assessing the influence of the polymer composition, it turns out that the incorporation of the aromatic PTH catalyst as the only hydrophobic side group is sufficient to induce the formation SCPNs without compromising the catalytic activity. Overall, these results are an important step towards a green and sustainable approach to conduct photoredox catalysis in aqueous media, which has tremendous potential for biological applications, decomposition of toxic and persistent halo-organic waste in water, or late-stage modifications of drugs. Future efforts in our research group will include the transformation of more demanding substrates, such as chlorides, with the power of light.

Experimental Section

General procedure for the dehalogenation reaction in water

A solution of 10 mg polymer in 0.8 mL of deionized water was charged with aryl iodide (30 µmol, 1.0 equiv.) and triethylamine (20.9 µL, 150 µmol, 5.0 equiv.). The mixture was irradiated with a 385 nm LED for 1 h while being stirred continuously and cooled by a stream of compressed air to keep it at room temperature. Afterwards, the aqueous mixture was extracted with CDCl₃ and the conversion was determined by ¹H NMR spectroscopy.

Acknowledgements

Conflict of interest

The authors declare no conflict of interest.

[1] N. A. Romero, D. A. Nicewicz, *Chem. Rev.* **2016**, *116*, 10075–10166.
[2] N. Corrigan, S. Shanmugam, J. Xu, C. Boyer, *Chem. Soc. Rev.* **2016**, *45*, 6165–6212.
[3] M. H. Shaw, J. Twilton, D. W. C. MacMillan, *J. Org. Chem.* **2016**, *81*, 6898–6926.
[4] L. Marzo, S. K. Pagire, O. Reiser, B. König, *Angew. Chem. Int. Ed.* **2018**, *57*, 10034–10072; *Angew. Chem.* **2018**, *130*, 10188–10228.
[5] B. H. Lipshutz, S. Ghorai, *Green Chem.* **2014**, *16*, 3660–3679.
[6] D. K. Romney, F. H. Arnold, B. H. Lipshutz, C.-J. Li, *J. Org. Chem.* **2018**, *83*, 7319–7322.

[7] D. Xue, Z.-H. Jia, C.-J. Zhao, Y.-Y. Zhang, C. Wang, J. Xiao, *Chem. Eur. J.* **2014**, *20*, 2960–2965.

[8] N. T. Vo, Y. Mekmouche, T. Tron, R. Guillot, F. Banse, Z. Halime, M. Sircoglou, W. Leibl, A. Aukauloo, *Angew. Chem. Int. Ed.* **2019**, *58*, 16023–16027; *Angew. Chem.* **2019**, *131*, 16169–16173.

[9] T. Kohlmann, R. Naumann, C. Kerzig, M. Goez, *Photochem. Photobiol. Sci.* **2017**, *16*, 1613–1622.

[10] R. Naumann, M. Goez, *Green Chem.* **2019**, *21*, 4470–4474.

[11] B. H. Lipshutz, S. Ghorai, M. Cortes-Clerget, *Chem. Eur. J.* **2018**, *24*, 6672–6695.

[12] M. Bu, C. Cai, F. Gallou, B. H. Lipshutz, *Green Chem.* **2018**, *20*, 1233–1237.

[13] M. Giedyk, R. Narobe, S. Weiß, D. Touraud, W. Kunz, B. König, *Nat. Catal.* **2020**, *3*, 40–47.

[14] C. Kerzig, M. Goez, *Chem. Sci.* **2016**, *7*, 3862–3868.

[15] R. Naumann, M. Goez, *Chem. Eur. J.* **2018**, *24*, 9833–9840.

[16] R. Naumann, F. Lehmann, M. Goez, *Angew. Chem. Int. Ed.* **2018**, *57*, 1078–1081; *Angew. Chem.* **2018**, *130*, 1090–1093.

[17] D. E. Bergbreiter, *Chem. Rev.* **2002**, *102*, 3345–3384.

[18] D. E. Bergbreiter, J. Tian, C. Hongfa, *Chem. Rev.* **2009**, *109*, 530–582.

[19] A. C. Albertsson, I. K. Varma, *Biomacromolecules* **2003**, *4*, 1466–1486.

[20] J. L. Hedrick, T. Magbitang, E. F. Connor, T. Glauser, W. Volksen, C. J. Hawker, V. Y. Lee, R. D. Miller, *Chem. Eur. J.* **2002**, *8*, 3308–3319.

[21] D. E. Bergbreiter, Y.-S. Liu, *Tetrahedron Lett.* **1997**, *38*, 7843–7846.

[22] D. E. Bergbreiter, Y.-S. Liu, *Tetrahedron Lett.* **1997**, *38*, 3703–3706.

[23] A. W. Bosman, R. Vestberg, A. Heumann, J. M. J. Fréchet, C. J. Hawker, *J. Am. Chem. Soc.* **2003**, *125*, 715–728.

[24] T. Terashima, M. Kamigaito, K.-Y. Baek, T. Ando, M. Sawamoto, *J. Am. Chem. Soc.* **2003**, *125*, 5288–5289.

[25] J. M. Ren, T. G. McKenzie, Q. Fu, E. H. H. Wong, J. Xu, Z. An, S. Shanmugam, T. P. Davis, C. Boyer, G. G. Qiao, *Chem. Rev.* **2016**, *116*, 6743–6836.

[26] D. Astruc, F. Chardac, *Chem. Rev.* **2001**, *101*, 2991–3024.

[27] L. J. Twyman, A. S. H. King, I. K. Martin, *Chem. Soc. Rev.* **2002**, *31*, 69–82.

[28] V. Rodionov, H. Gao, S. Scroggins, D. A. Unruh, A.-J. Avestro, J. M. J. Fréchet, *J. Am. Chem. Soc.* **2010**, *132*, 2570–2572.

[29] C. Deraedt, N. Pinaud, D. Astruc, *J. Am. Chem. Soc.* **2014**, *136*, 12092–12098.

[30] X. Liu, D. Gregurec, J. Irigoyen, A. Martinez, S. Moya, R. Ciganda, P. Hermange, J. Ruiz, D. Astruc, *Nat. Commun.* **2016**, *7*, 13152.

[31] Y. Liu, Y. Wang, Y. Wang, J. Lu, V. Piñón, M. Weck, *J. Am. Chem. Soc.* **2011**, *133*, 14260–14263.

[32] J. Lu, J. Dimroth, M. Weck, *J. Am. Chem. Soc.* **2015**, *137*, 12984–12989.

[33] L.-C. Lee, J. Lu, M. Weck, C. W. Jones, *ACS Catal.* **2016**, *6*, 784–787.

[34] S. Handa, D. J. Lippincott, D. H. Aue, B. H. Lipshutz, *Angew. Chem. Int. Ed.* **2014**, *53*, 10658–10662; *Angew. Chem.* **2014**, *126*, 10834–10838.

[35] S. Handa, E. D. Slack, B. H. Lipshutz, *Angew. Chem. Int. Ed.* **2015**, *54*, 11994–11998; *Angew. Chem.* **2015**, *127*, 12162–12166.

[36] H. Pang, Y. Wang, F. Gallou, B. H. Lipshutz, *J. Am. Chem. Soc.* **2019**, *141*, 17117–17124.

[37] A. Lu, D. Moatsou, D. A. Longbottom, R. K. O'Reilly, *Chem. Sci.* **2013**, *4*, 965–969.

[38] B. L. Moore, D. Moatsou, A. Lu, R. K. O'Reilly, *Polym. Chem.* **2014**, *5*, 3487–3494.

[39] W. J. Shaw, J. C. Linehan, A. Gutowska, D. Newell, T. Bitterwolf, J. L. Fulton, Y. Chen, C. F. Windisch, *Inorg. Chem. Commun.* **2005**, *8*, 894–896.

[40] Y. Arakawa, A. Chiba, N. Haraguchi, S. Itsuno, *Adv. Synth. Catal.* **2008**, *350*, 2295–2304.

[41] T. Terashima, T. Mes, T. F. A. De Greef, M. A. J. Gillissen, P. Besenius, A. R. A. Palmans, E. W. Meijer, *J. Am. Chem. Soc.* **2011**, *133*, 4742–4745.

[42] E. Huerta, P. J. M. Stals, E. W. Meijer, A. R. A. Palmans, *Angew. Chem. Int. Ed.* **2013**, *52*, 2906–2910; *Angew. Chem.* **2013**, *125*, 2978–2982.

[43] Y. Liu, S. Pujals, P. J. M. Stals, T. Paulöhrl, S. I. Presolski, E. W. Meijer, L. Albertazzi, A. R. A. Palmans, *J. Am. Chem. Soc.* **2018**, *140*, 3423–3433.

[44] E. H. Discekici, N. J. Treat, S. O. Poelma, K. M. Mattson, Z. M. Hudson, Y. Luo, C. J. Hawker, J. R. de Alaniz, *Chem. Commun.* **2015**, *51*, 11705–11708.

[45] S. O. Poelma, G. L. Burnett, E. H. Discekici, K. M. Mattson, N. J. Treat, Y. Luo, Z. M. Hudson, S. L. Shankel, P. G. Clark, J. W. Kramer, C. J. Hawker, J. Read de Alaniz, *J. Org. Chem.* **2016**, *81*, 7155–7160.

[46] N. J. Treat, H. Sprafke, J. W. Kramer, P. G. Clark, B. E. Barton, J. Read de Alaniz, B. P. Fors, C. J. Hawker, *J. Am. Chem. Soc.* **2014**, *136*, 16096–16101.

[47] J. Yan, X. Pan, M. Schmitt, Z. Wang, M. R. Bockstaller, K. Matyjaszewski, *ACS Macro Lett.* **2016**, *5*, 661–665.

[48] J. Wang, L. Yuan, Z. Wang, M. A. Rahman, Y. Huang, T. Zhu, R. Wang, J. Cheng, C. Wang, F. Chu, C. Tang, *Macromolecules* **2016**, *49*, 7709–7717.

[49] S. Dadashi-Silab, X. Pan, K. Matyjaszewski, *Chem. Eur. J.* **2017**, *23*, 5972–5977.

[50] H. Zhang, J. Hui, H. Chen, J. Chen, W. Xu, Z. Shuai, D. Zhu, X. Guo, *Adv. Electron. Mater.* **2015**, *1*, 1500159.

[51] Y. Liang, D. E. Bergbreiter, *Polym. Chem.* **2016**, *7*, 2161–2165.

[52] G. M. ter Huurne, L. N. J. de Windt, Y. Liu, E. W. Meijer, I. K. Voets, A. R. A. Palmans, *Macromolecules* **2017**, *50*, 8562–8569.

[53] M. A. J. Gillissen, T. Terashima, E. W. Meijer, A. R. A. Palmans, I. K. Voets, *Macromolecules* **2013**, *46*, 4120–4125.

[54] J. Choi, P. Schattling, F. D. Jochum, J. Pyun, K. Char, P. Theato, *J. Polym. Sci. Part A* **2012**, *50*, 4010–4018.

[55] Y. Hirai, T. Terashima, M. Takenaka, M. Sawamoto, *Macromolecules* **2016**, *49*, 5084–5091.

[56] G. Hattori, Y. Hirai, M. Sawamoto, T. Terashima, *Polym. Chem.* **2017**, *8*, 7248–7259.

[57] Y. Morishima, S. Nomura, T. Ikeda, M. Seki, M. Kamachi, *Macromolecules* **1995**, *28*, 2874–2881.

[58] A. Steiner, J. D. Williams, J. A. Rincón, O. de Frutos, C. Mateos, C. O. Kappe, *Eur. J. Org. Chem.* **2019**, 5807–5811.

[59] I. Ghosh, T. Ghosh, J. I. Bardagi, B. König, *Science* **2014**, *346*, 725–728.

[60] J. I. Bardagi, I. Ghosh, M. Schmalzbauer, T. Ghosh, B. König, *Eur. J. Org. Chem.* **2018**, 34–40.

[61] N. G. W. Cowper, C. P. Chernowsky, O. P. Williams, Z. K. Wickens, *J. Am. Chem. Soc.* **2020**, *142*, 2093–2099.